

Large Co Cluster Deposition on Naturally and Artificially Patterned Substrates

This content has been downloaded from IOPscience. Please scroll down to see the full text.

2002 Jpn. J. Appl. Phys. 41 5726

(<http://iopscience.iop.org/1347-4065/41/9R/5726>)

View [the table of contents for this issue](#), or go to the [journal homepage](#) for more

Download details:

IP Address: 59.77.20.112

This content was downloaded on 06/11/2014 at 12:09

Please note that [terms and conditions apply](#).

Large Co Cluster Deposition on Naturally and Artificially Patterned Substrates

Dong-Liang PENG^{1,2*}, Gilles LERONDEL^{3†}, Takehiko HIHARA¹, Kenji SUMIYAMA¹ and Takafumi YAO³

¹Department of Materials Science and Engineering, Nagoya Institute of Technology, Nagoya 466-8555, Japan

²Japan Society for the Promotion of Science (JSPS), 6 Ichibancho, Chiyoda-ku, Tokyo 102-8471, Japan

³Institute for Materials Research, Tohoku University, 2-1-1 Katahira, Aoba-ku, Sendai 980-8577, Japan

(Received January 22, 2002; revised manuscript received May 7, 2002; accepted for publication May 22, 2002)

Monodispersed Co clusters with mean cluster diameter $d = 13$ nm have been deposited on a stepped graphite surface and a lithography-patterned Si wafer using a plasma-gas-condensation cluster beam deposition apparatus. High-resolution scanning electron microscope observation indicates that 1) cluster aggregation is much more limited at the steps than on the flat terrace regions of the graphite surface, and 2) cluster density is much higher in the grooves than on the flat top of the lithography-patterned Si wafers. These results suggest the possibility of the regular arrangement of monodispersed Co clusters if the pattern size (the width of grooves and tops) is comparable with the cluster size. [DOI: 10.1143/JJAP.41.5726]

KEYWORDS: Co cluster, cluster beam deposition, regular arrangement, lithography, mobility

1. Introduction

For future application of highly dense storage media or advanced electronics and photonics devices, nanoscale controlled dot and wire arrays have been fabricated via a top-down route of lithography combined with artificial superlattice deposition.¹⁾ Periodical lattice and/or self-assemblies of nanoparticles have also been widely prepared via a bottom-up route using colloidal solutions and controlling interaction of surfactants.²⁾ Since we have been able to produce monodispersed size clusters with standard deviation (Δ) less than 10% of the mean diameter (d) via another bottom-up route of condensing vaporized atoms in clean inert gas atmosphere,³⁾ we attempt to deposit these clusters in a specific ordered manner.

A number of workers have explored the formation of clusters at steps via atomic vapor deposition.^{4–7)} Experimental studies of atom and dimer diffusion along step edges,^{8,9)} and theoretical studies of island growth on steps in epitaxial systems¹⁰⁾ have also been reported. There are also several reports on the size-selected cluster deposition of silver (Ag₅₀, Ag₁₈₅, Ag₂₅₀ and Ag₄₀₀) on a graphite surface using the cluster beam deposition method.^{11,12)} Since the small Ag clusters deposited on the graphite surface can diffuse across the surface and aggregate into larger particles ($d \approx 14$ nm), the benefit of the size-selective cluster beams is lost. In this paper, we report the deposition of large size-monodispersed Co clusters ($d = 13$ nm) onto a graphite substrate with steps and a silicon substrate with grooves.

2. Experimental

The monodispersed Co clusters were prepared using the plasma-gas-condensation (PGC) cluster beam deposition apparatus, the details of which have been described elsewhere.^{13,14)} The apparatus is composed of three main parts: a sputtering chamber, a cluster growth room and a deposition chamber. The sample substrate can be heated to 500°C using a resistive heater and is fixed onto the sample holder in the deposition chamber. The clusters were deposited onto highly oriented pyrolytic graphite (HOPG)

substrates and lithograph-patterned Si wafers in a high-vacuum chamber with a background pressure of 10^{-8} – 10^{-7} Torr; during deposition the pressure in the deposition chamber rose to 10^{-5} Torr owing to remaining Ar gas. The cluster deposition rate, $r_d = 2$ – 3.5 nm/min, was estimated using a quartz thickness monitor and by measuring the weight of the deposited clusters. The size of clusters deposited on microgrids was estimated using a Hitachi HF-2000 transmission electron microscope (TEM), operating at 200 kV. The morphology of clusters deposited on the HOPG and patterned Si substrates was observed using a high-resolution scanning electron microscope (SEM) (JEOL: JSM-6320F) operating at 3 kV.

3. Results and Discussion

Figure 1 shows (a) bright-field TEM images and (b) corresponding cluster size distributions of Co clusters deposited on a microgrid at room temperature and Ar gas flow rate $R_{Ar} = 500$ sccm. Here, we estimated the cluster size distributions from digitized images recorded by a slow-scan charge-coupled device (CCD) camera in the object area of 350×350 nm² using image-analysis software (Image-Pro PLUS: Media Cybernetics). These figures clearly indicate the formation of size-monodispersed clusters with the mean diameter (d) of about 13 nm and standard deviation (Δ) less than 10% of the mean size. Moreover, individual Co clusters can be distinguished in spite of their partial overlap. This suggests that the cluster size in the cluster beam is maintained on the substrate.

Figure 2 shows the SEM images observed at room temperature after depositing the monodispersed Co clusters onto stepped HOPG substrates (deposition rate: $r_d = 2.5$ nm/min; deposition time: $t_d = 1$ min). The substrate temperature, $T_s = 27, 100, 200,$ or 300°C , held only during the deposition time and then was decreased to room temperature. The clusters are observed on both terraces and steps. Clearly, the number of Co clusters observed in the step regions is more than that in the terrace regions. This feature becomes more conspicuous with increasing substrate temperature. These observations suggest that large Co clusters of $d = 13$ nm are able to diffuse across terraces even at room temperature and are trapped at the steps; high substrate temperature is effective for increasing the mobility or diffusion of the Co clusters on the substrate. Here, we

*E-mail: pengdl@mse.nitech.ac.jp

†Permanent address: Laboratoire de Nanotechnologie et d'Instrumentation Optique, Université de Technologie de Troyes, Troyes 10010, BP 2060, France.

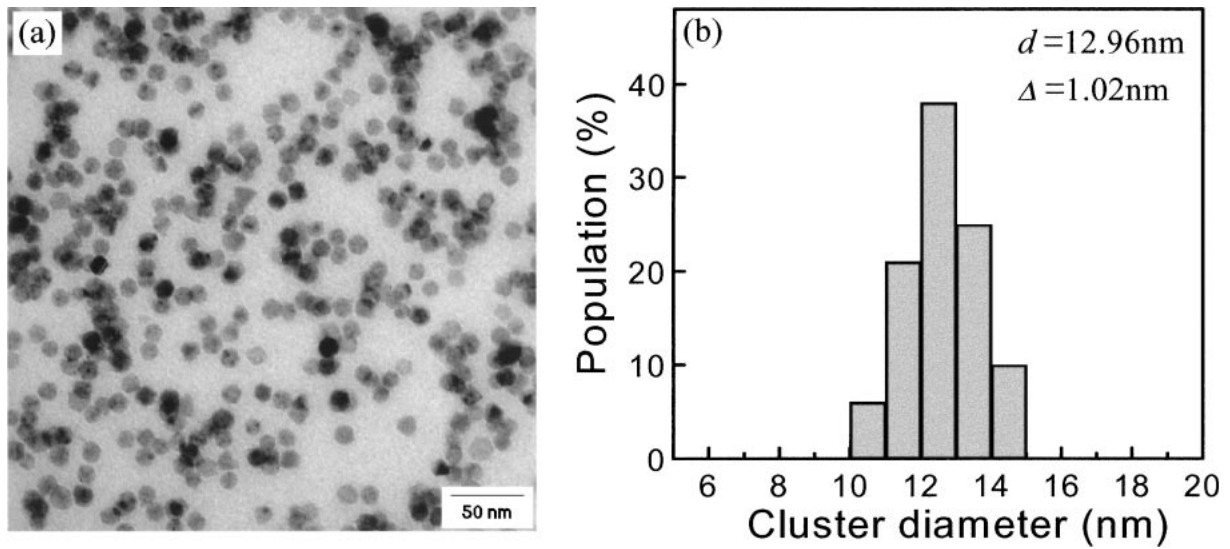


Fig. 1. (a) TEM image and (b) cluster size distribution of monodispersed Co clusters deposited onto a carbon microgrid at $T_s = 27^\circ\text{C}$ and Ar gas flow rate $R_{\text{Ar}} = 500$ sccm.

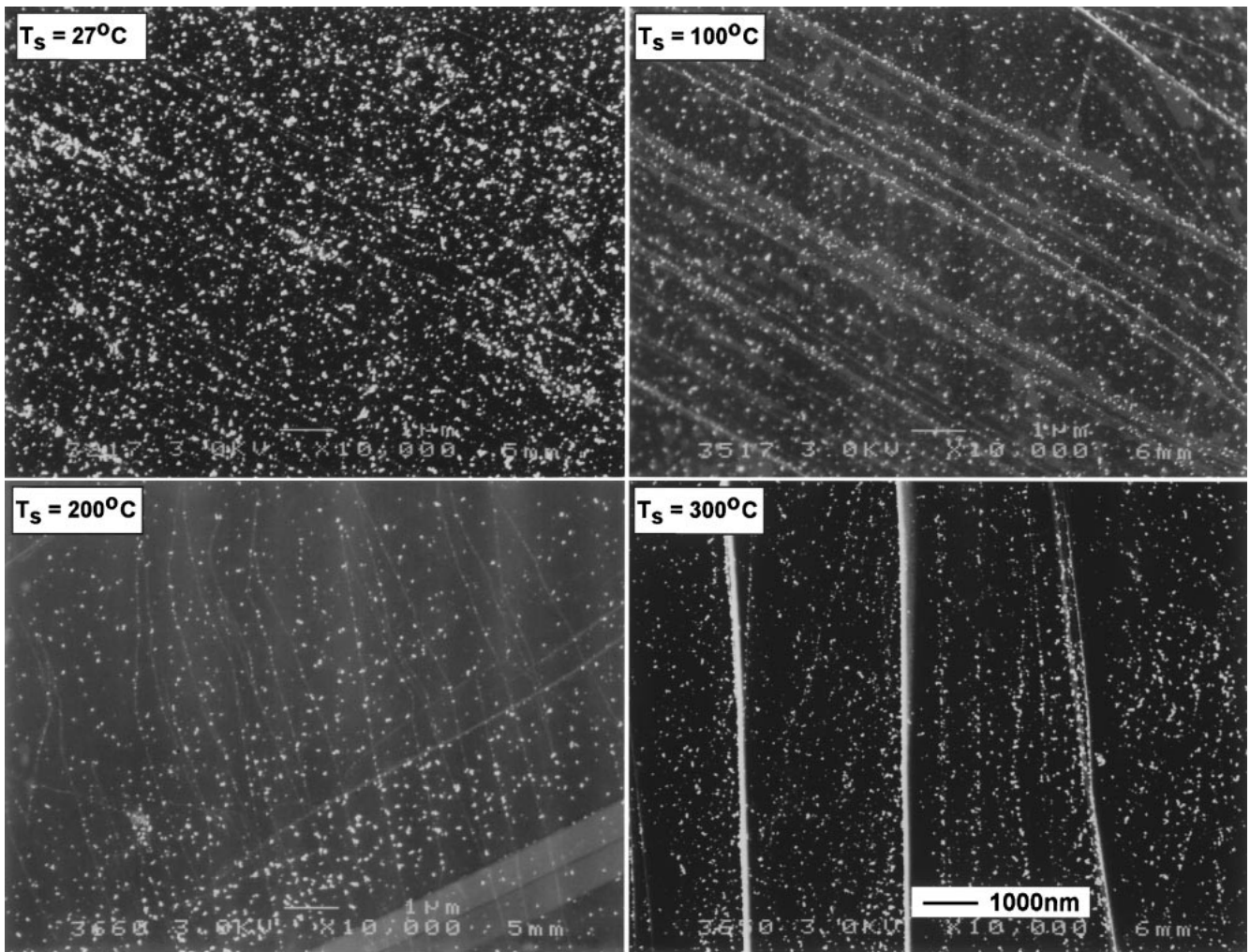


Fig. 2. SEM images observed at room temperature after depositing Co clusters onto stepped HOPG substrates (deposition rate: $r_d = 2.5$ nm/min) kept at $T_s = 27, 100, 200,$ and 300°C .

have to consider cluster-cluster coalescence behavior. Our previous electrical conductivity measurement and TEM observation studies¹⁵⁾ on the coalescence process revealed

that cluster-cluster coalescence begins at their interface at $T > 100^\circ\text{C}$, while the morphology of cluster distribution shows no marked change at substrate temperatures $T_s <$

250°C for Co clusters with $d = 8.5$ nm. When $T_s > 250^\circ\text{C}$, the morphology of the cluster distribution is considerably changed and intercluster coalescence and the growth or reconstruction of neighboring clusters is detectable. We suggest that a substrate temperature below 250°C is suitable for promoting cluster migration while maintaining their original size and structure.

As seen in Fig. 2, Co clusters are more effectively trapped at the steps than on the flat terrace regions of the HOPG substrate. However, the step directions are not regular on natural HOPG surfaces. In order to fabricate regular arrays of monodispersed Co clusters, we used lithography-patterned Si wafer substrates. The grooves made by lithography have a V shape. Figures 3(a) and 3(b) show atomic force microscope (AFM) images of the cross-sectional structure and size of the lithography-patterned Si wafer, and of the cluster distribution after depositing Co

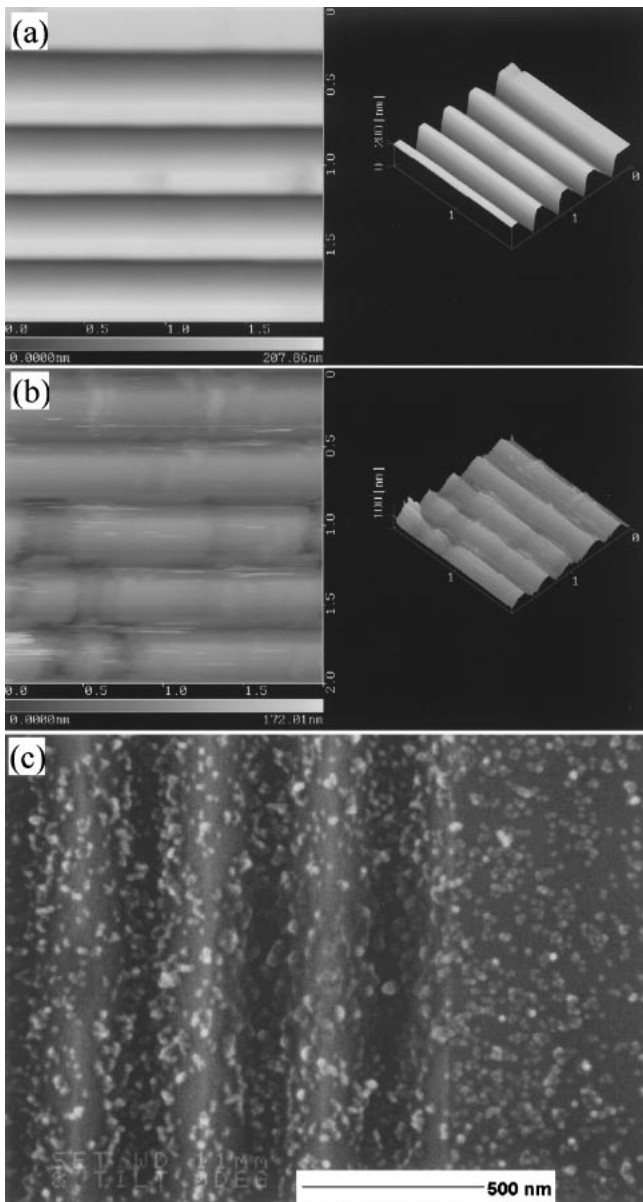


Fig. 3. (a) AFM image of the cross-sectional structure and size of lithography-patterned Si wafer; (b) AFM image of the cluster distribution after depositing Co clusters at room temperature (deposition rate: $r_d = 2.5$ nm/min) onto this wafer; (c) SEM image of the same sample.

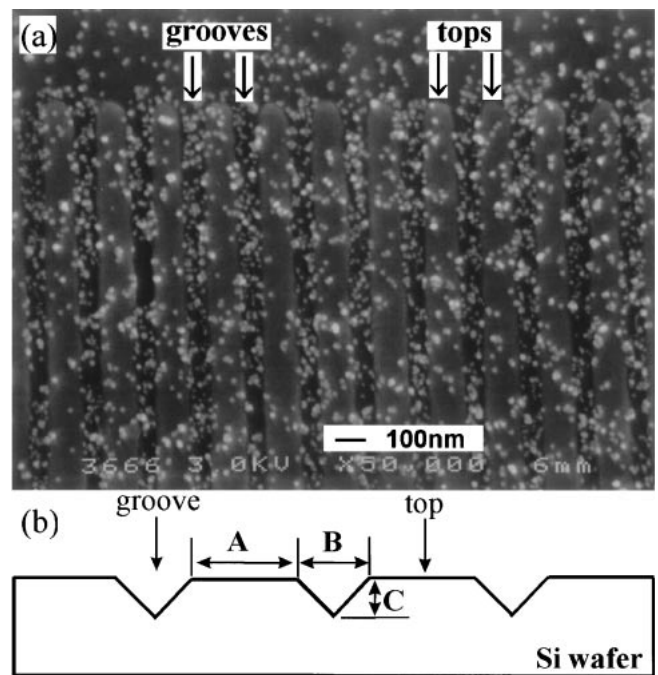


Fig. 4. (a) SEM images observed at room temperature after depositing Co clusters onto lithography-patterned Si wafer (deposition rate: $r_d = 2.5$ nm/min) kept at $T_s = 200^\circ\text{C}$; (b) a schematic drawing of the cross-sectional structure and size of lithography-patterned Si wafer.

clusters onto this wafer at room temperature (deposition rate: $r_d = 2.5$ nm/min; deposition time: $t_d = 1$ min). Figure 3(c) shows a SEM image of the same sample. From Figs. 3(b) and 3(c), although a higher cluster density is observed inside the grooves, the pattern size is too large in comparison with the cluster size to clearly observe selective growth. Thus, we further decreased the pattern size and increased the substrate temperature. Figure 4 shows (a) SEM images observed at room temperature after depositing Co clusters (deposition rate: $r_d = 2.5$ nm/min) onto the lithography-patterned Si wafer kept at $T_s = 200^\circ\text{C}$, and (b) a schematic drawing of the cross-sectional structure and size of the lithography-patterned Si wafer. The pattern parameter is $A/B/C = 100/80/50$ nm. From Fig. 4(a), due to cluster migration, a much higher cluster density is observed inside the grooves than on the tops. This clearly indicates that the grooves act as effective sites for Co cluster assembly. In other words, the mobility of the clusters is greatly reduced at the grooves. On the other hand, we also see a small number of incident Co clusters on the tops, suggesting that those clusters are trapped at defect sites on the tops and/or the pattern size of the Si wafer is still too large to induce selective regular distribution of clusters. We aim to obtain a Si wafer substrate with a smaller pattern size, though it is difficult to process a smaller size pattern on a substrate by lithography.

As described above, large Co clusters ($d = 13$ nm) containing about 10^5 atoms also have high mobility, similar to antimony clusters (~ 2300 atoms, $d = 5$ nm).¹⁶⁾ For antimony clusters on graphite, a surprisingly high cluster mobility has also been observed,¹⁶⁾ which could not be accounted for by the atomic processes of edge diffusion,¹⁷⁾ and evaporation and subsequent condensation of their peripheral atoms¹⁸⁾ because of their diffusion coefficient $D = D_0 \exp(-E_a/k_B T)$ with $D_0 \approx 1.6 \times 10^4$ cm²/s and acti-

vation energy $E_a = 0.7 \pm 0.1$ eV. If diffusion is limited by the migration of one atom from the bulk to the surface, $D_0 \approx 10^{-3}$ cm²/s is observed.^{4,17,19)} Therefore, high cluster mobility should result from the collective motion of all atoms of a cluster. Recently, this fast diffusion or high mobility has been described as a Brownian motion induced by the internal vibrations of the cluster and/or the vibrations of the substrate, in a molecular dynamics study of large Lennard-Jones clusters evolving on a crystalline surface.²⁰⁾ When the cluster is not commensurate with the substrate, the interaction felt by the cluster center of mass is small. In this case, the cluster is not locked by the substrate and can vibrate relatively freely. Both the internal vibrations of the cluster and the vibrations of the substrate create a random force on the cluster center of mass, which induces a Brownian motion in this weak external potential. This random force is sufficiently strong to overcome the small energy barriers, resulting in a rapid diffusive motion. Quite recently, through extensive molecular dynamics simulations, Luedtke and Landman²¹⁾ reported another collective diffusion mechanism, slip diffusion, of a gold cluster (Au₁₄₀) adsorbed on a graphite surface, which involves long sliding trajectories, which may be described mathematically as Levy flight.²²⁾ For the present large Co clusters, it is difficult to imagine that such a Brownian motion and slip diffusion also result in high mobility. As can be seen in Fig. 1, most Co clusters have a spherical shape. We believe that in this case, rotation of the clusters on the substrate may give an important contribution to the high mobility.

In order to further discuss the possibility of regular arrangement of monodispersed Co clusters, we estimate the diffusion length (L_D) using the above-mentioned diffusion coefficient (D) and activation energy (E_a) of antimony clusters and the following equation:

$$L_D = (Dt)^{1/2}, \quad (1)$$

where t is diffusion time. If we take $t = 1$ s (the deposition time of the sample is about 1 min), then we can obtain the diffusion lengths $L_D = 1.69 \times 10^3$, 2.38×10^4 , 2.37×10^5 , and 1.06×10^6 nm for $T_s = 27$, 100, 200, and 300°C, respectively. Clearly, these values are much longer than the widths (10^2 – 10^3 nm) of terraces on the stepped HOPG substrates and the tops of lithography-patterned Si wafer substrates. For example, L_D is larger by two or three orders of magnitude than the widths of the terraces and tops at $T_s = 200^\circ\text{C}$. This also suggests that the clusters can move into the grooves and are trapped there. However, as seen in Figs. 2 and 4, only a locally regular arrangement of Co clusters is observed. There are some reasonable explanations for this. In this estimation, we first used the values of D and E_a of the antimony clusters for the estimation of L_D , while the present Co clusters ($d = 13$ nm) are much larger than the antimony clusters ($d = 5$ nm), and thus the values of D should be much smaller than those for the antimony clusters. Secondly, since the defect sites and/or roughness of the terraces (HOPG) and tops (lithography-patterned Si wafer) trap the migrating clusters, they prevent the regular arrangement of clusters on the steps and grooves. They also lead to the presence of a small number of Co clusters on the terraces and tops. Thirdly, it should be noted that at

$T_s = 27^\circ\text{C}$ (Fig. 3) and 200°C (Fig. 4), “large clusters” formed by connection and/or overlap of several incident clusters are often observed on the tops and in the grooves. Moreover, at $T_s = 200^\circ\text{C}$, cluster-cluster coalescence takes place at their interface¹⁵⁾ though the high substrate temperature is effective for increasing the mobility of clusters. The formation of such a “large random network cluster” also prevents the regular arrangement of Co clusters on the grooves. To solve this problem, we must adopt slow cluster deposition (namely, a very low deposition rate) and ensure sufficient time for clusters to migrate into a groove before two clusters meet each other on the top of substrates.

4. Conclusions

We have demonstrated the deposition of large Co clusters on a stepped graphite surface and a lithography-patterned Si wafer. High mobility of the Co clusters is observed. Cluster migration is much more limited at the grooves than on the top of the lithography-patterned Si wafer, leading to a much higher cluster density in the grooves. These results suggest the possibility of the fabrication of size-monodispersed Co clusters in a regular arrangement.

Acknowledgments

This work has been supported by Core Research for Evolutional Science and Technology (CREST) of Japan Science and Technology Corporation (JST). Two of the authors (D. L. Peng and G. Lerondel) appreciate the financial support from Japan Society for the Promotion of Science (JSPS).

- 1) M. Zheng, M. Yu, Y. Liu, R. Skomski, S. H. Liou, D. J. Sellmyer, V. N. Petryakov, Yu. K. Verevkin, N. I. Polushkin and N. N. Salashchenko: *Appl. Phys. Lett.* **79** (2001) 2606.
- 2) C. T. Black, C. B. Murray, R. L. Sandstrom and S. Sun: *Science* **290** (2000) 1131.
- 3) S. Yamamuro, K. Sumiyama and K. Suzuki: *J. Appl. Phys.* **85** (1999) 483.
- 4) A. D. Gates and J. L. Robins: *Surf. Sci.* **116** (1982) 188.
- 5) A. D. Gates and J. L. Robins: *Surf. Sci.* **191** (1987) 492.
- 6) A. D. Gates and J. L. Robins: *Surf. Sci.* **191** (1987) 499.
- 7) G. M. Francis, L. Kuipers, J. R. A. Cleaver and R. E. Palmer: *J. Appl. Phys.* **79** (1996) 2942.
- 8) G. L. Kellogg: *Surf. Sci.* **359** (1996) 237.
- 9) T. Y. Fu, Y. R. Tzeng and T. T. Tsong: *Surf. Sci.* **366** (1996) L691.
- 10) J. A. Blackman and P. A. Mulheran: *Phys. Rev. B* **54** (1996) 11681.
- 11) I. M. Goldby, L. Kuipers, B. von Issendorff and R. E. Palmer: *Appl. Phys. Lett.* **69** (1996) 2819.
- 12) S. J. Carroll, K. Seeger and R. E. Palmer: *Appl. Phys. Lett.* **72** (1998) 305.
- 13) S. Yamamuro, K. Sumiyama, M. Sakurai and K. Suzuki: *Supramol. Sci.* **5** (1998) 239.
- 14) S. Yamamuro, K. Sumiyama, M. Sakurai and K. Suzuki: *Eur. Phys. J. D* **9** (1999) 575.
- 15) D. L. Peng, T. J. Konno, K. Wakoh, T. Hihara and K. Sumiyama: *Appl. Phys. Lett.* **78** (2001) 1535.
- 16) L. Bardotti, P. Jensen, A. Hoareau, M. Treilleux and B. Cabaud: *Phys. Rev. Lett.* **74** (1995) 4694.
- 17) G. L. Kellogg: *Phys. Rev. Lett.* **73** (1994) 1833.
- 18) J.-M. Wen, S.-L. Chang, J. W. Burnett, J. W. Evans and P. A. Thiel: *Phys. Rev. Lett.* **73** (1994) 2591.
- 19) A. F. Voter: *Phys. Rev. B* **34** (1986) 6819.
- 20) P. Deltour, J.-L. Barrat and P. Jensen: *Phys. Rev. Lett.* **78** (1997) 4597.
- 21) W. D. Luedtke and U. Landman: *Phys. Rev. Lett.* **82** (1999) 3835.
- 22) J.-P. Bouchaud and A. Georges: *Phys. Rep.* **4–5** (1990) 127.